



Emergence of Oblong School Shape: Models and Empirical Data of Fish

Charlotte K. Hemelrijk, Hanno Hildenbrandt, José Reinders & Eize J. Stamhuis

Behavioural Ecology and Self-organisation, Marine Biology, Centre for Ecological and Evolutionary Studies, University of Groningen, Groningen, The Netherlands

Correspondence

C. K. Hemelrijk, Behavioural Ecology and Self-organisation, Marine Biology, Centre for Ecological and Evolutionary Studies, University of Groningen, Groningen, The Netherlands.
E-mail: c.k.hemelrijk@rug.nl

Received: January 6, 2010

Initial acceptance: February 28, 2010

Final acceptance: July 19, 2010

(K. Reinhold)

doi: 10.1111/j.1439-0310.2010.01818.x

Abstract

The main benefit of the oblong shape of schools of fish is supposed to be the protection against predation. Models of self-organised travelling groups have shown that this shape may arise as a side effect of the avoidance of collisions with group members. These models were developed for schools of fish in open water, whereas the oblong shape of schools of real fish has mostly been observed in schools in tanks. Therefore, it is not known how school shape in a tank originates neither in models nor in real fish. To find out what causes this shape, we use the combination of a theoretical and an empirical study. We test the predictions produced by our earlier models regarding the effect of school size on the school shape both in a model of self-organised schooling in a tank and empirically. Empirically, we study the 3D positions of all individuals in the schools of 10–60 real mullets (*Chelon labrosus*). We calculate for each individual its distance to its nearest neighbour and its velocity and we measure per school its length and width. The relation between school shape and size in the model and in the real mullets supports our prediction and thus supports the hypothesis that school shape may be emergent from the avoidance of collisions during coordinated travelling.

Introduction

Most fish have the habit of schooling (Krause & Ruxton 2002). The main function of schooling is said to be the reduction in predation (Krause & Ruxton 2002). Several theoretical papers have suggested that the optimal shape for a school of fish should be spherical, because it is the form with the smallest surface and the greatest volume and therefore a spherical school should run the smallest risk of being discovered by a predator (Breder 1959, 1976; Cushing & Harden-Jones 1968; Hamilton 1971; Radakov 1973). However, the shape of schools is rarely spherical, it appears usually to be oblong, thus, longer than wide (Partridge et al. 1980; Pitcher 1986). Yet again, the benefit of the oblong shape is considered to be the protection against predators. Predators are supposed to attack from the front, and

therefore, the front of the school should be narrow (Bumann et al. 1997). However, the causes of school shape are still unknown: no detailed empirical study exists.

In models of travelling schools, the oblong shape emerges by self-organisation as a side effect of the movement, coordination and collision avoidance of the individuals (Hemelrijk & Kunz 2005; Hemelrijk & Hildenbrandt 2008). The coordinated movement of groups is modelled by means of three rules: (1) that individuals are cohering with others further away; (2) that they align with others at intermediate distance; and (3) that they move away from those that are close by (Huth & Wissel 1992, 1994; Reuter & Breckling 1994; Couzin et al. 2002; Couzin & Krause 2003; Kunz & Hemelrijk 2003; Hemelrijk & Kunz 2005; Parrish & Viscido 2005; Hemelrijk & Hildenbrandt 2008).

However, this model-generated explanation of the oblong shape has been derived from free-swimming fish (Hemelrijk & Hildenbrandt 2008), whereas most empirical data refer to fish in a tank (Partridge 1980; Partridge et al. 1980). Therefore, it is uncertain whether this explanation is relevant also for schools in a tank. In a tank, apart from coordinating their movement with others, individuals must also avoid walls and this may influence the shape of the school, just as attraction to a sleeping site does in our starling model (Hildenbrandt et al. in press). Here, we combine a modelling study of self-organised schooling in a tank with an empirical study of the three-dimensional location of individuals in schools of mullets (*Chelon labrosus*). The added value of combining a theoretical and empirical study clearly appears from numerous earlier studies related to several data, e.g. of fish and birds (Huth & Wissel 1994; Grünbaum 1998; Huse et al. 2002; Couzin et al. 2005; Becco et al. 2006; Biro et al. 2006; Barbaro et al. 2009; Ward et al. 2008; Faria et al. 2009), wildebeest (Gueron & Levin 1993) and locusts and crickets (Vicsek et al. 1995; Buhl et al. 2006; Faria et al. 2009; Yates et al. 2009) (Simpson et al. 2006; Bazazi et al. 2008; Romanczuk et al. 2009).

In the present study, we want to evaluate our previous explanations regarding the causation of school shape (Hemelrijk & Hildenbrandt 2008). Our former models suggested that an oblong shape develops through collision avoidance in a moving group by the following process (Kunz & Hemelrijk 2003; Hemelrijk & Kunz 2005; Hemelrijk & Hildenbrandt 2008): In Fig. 1a, at time $t = 1$, the black individual slows down to avoid a collision. Thus, at time $t = 2$, the

school lengthens, while the gap between its former neighbours is filled by the inward movement of these neighbours. Therefore, at the time $t = 3$, the school becomes narrower. Thus, the school becomes oblong. Although to verify this explanation directly is difficult, both in the model and empirically, the explanation is supported by four patterns that can be tested easily. They result from school size and speed (Fig. 1b) (Hemelrijk & Hildenbrandt 2008): Larger schools are (1) denser and (2) more oblong (Hyp1, Hyp 2 in Fig. 1b). Higher density in larger schools (on average and also in their interior, i.e. the densest core, Hemelrijk & Hildenbrandt 2008) arises from the increase in attraction caused by the higher number of individuals. Denser schools are more elongated because the greater density leads to a higher number of movements to avoid collisions. Further, compared to fast schools, slower schools are (3) less polarised and (4) more oblong (Hyp3, Hyp4 in Fig. 1b). Weaker polarisation in slower schools is because of less resistance to turn, i.e. less inertia. Therefore, it leads to more events of collision avoidance and thus to the lengthening of the school. This model-based explanation of school shape holds in several models despite differences in details of the three behavioural rules (Kunz & Hemelrijk 2003; Hemelrijk & Kunz 2005; Hemelrijk & Hildenbrandt 2008).

Although the four patterns indicated previously (Fig. 1b) have as yet not been studied systematically empirically, there are indications in support of each of them. Several studies show that the density is higher (as revealed by the reduced distance to the nearest neighbours) when the school size is larger (Breder 1954; Keenleyside 1955; Nursall 1973;

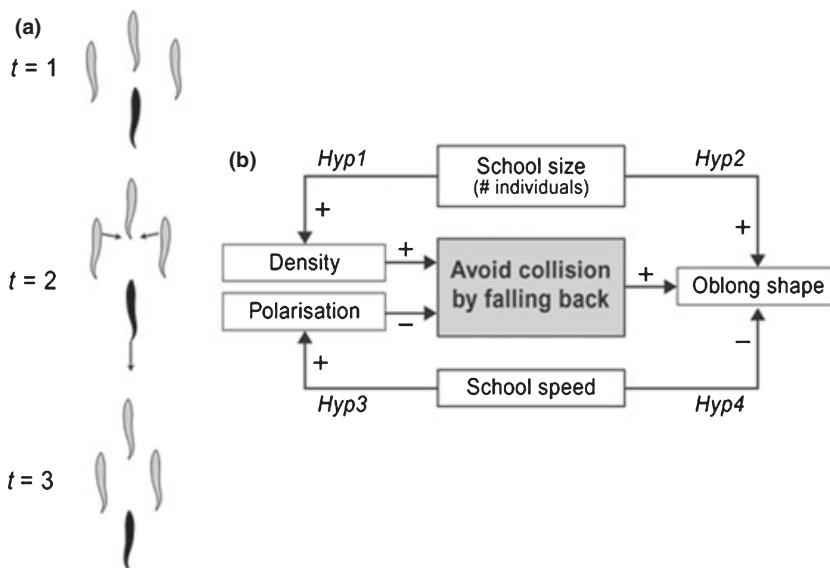


Fig. 1: The supposed causation of the oblong shape of a school. (a) School shape and avoidance of collision by slowing down while moving. (b) the four interconnecting patterns related with school size (# school members) and speed. Hyp is an abbreviation of hypothesis.

Partridge 1980; Partridge & Pitcher 1980; Becco et al. 2006). The positive correlation between the number of individuals and the oblong shape has been mentioned for herring *Clupea harengus* (Axelsen et al. 2001). That slower schools are more oblong has been reported for cod and saithe by Partridge and co-authors (Partridge et al. 1980), but this contradicted the theoretical predictions by Breder (Breder 1959) and Radakov (Radakov 1973). Further, for small schools of eight Danios, there is evidence that greater speed is accompanied by stronger polarisation (Viscido et al. 2004).

We investigate in the present study whether the two patterns related to group size shown in Fig. 1b hold also in a model of schools in a tank and in empirical data in a tank (Hemelrijk & Hildenbrandt 2008). We have extended our former model of self-organised schools by placing the school in a tank and supplying individuals with extra rules to avoid colliding with the walls. We model a tank that is identical in size and shape to the one used in our empirical study; we develop rules of wall avoidance and tune parameters so that the trajectories of the school in the model resemble those of the empirical study. In our empirical study, we use mullets, a species that schools both in captivity and in the wild (Videler 1993). By means of mirrors and several video cameras, we determine the 3D positions of the fish and measure the shape (length and width) and the internal structure (NND and polarisation) of mullet schools ranging from 10 to 60 individuals.

Our results confirm the predictions produced by our earlier models. This indicates that similar processes cause the school form to become oblong in schools of both the modelled individuals and real mullets moving in a tank. We indicate areas of future study.

Methods

Experiments and Data Collection

The fish and the tank

We have studied thick-lipped grey mullets (*Chelon labrosus*). Individuals were fed every second day, but not on experimental days. They were kept in a tank with a height of 0.8 m. The tank had a shape of an octagonal ring with an outer diameter of 3 m and a central 'hole' with a diameter of 1 m and (Fig. 2a,b). The tank contained approximately 6000 l of seawater produced from demineralised water and artificial sea salt

(Aqua Medic) in a concentration of 3.0%. The light dark regime of the normal neon light illumination was 12-h light alternating with 12-h darkness (12L/12D). To generate an even illumination over the whole tank during experimental recordings, the tank was illuminated at four places also by halogen flood lights of 150 W each (Fig. 2a). At one side of the tank, the width of the passage was reduced by a double wall with a mirror. Therefore, we call it the 'narrow passage'. This mirror we needed for estimating the three-dimensional positions of the fish. The opposite passage that lacked such obstruction will be indicated as the 'wide passage'. The shortest passage we refer to as the 'corner' (Fig. 2a).

The Experimental Procedure, Recordings and Data-Processing

To record the trajectories of the fish schools, four cameras (Bascom IR-30 wireless) were mounted above the tank (Fig. 2a). Their fields of view covered half the entire tank around the wide passage.

To measure the 3D positions of all individual fish in a school, we used video recordings of the schools in the narrow passage. In these recordings, we combined positional measurements taken by direct observations of the fish with those from their images in the mirror (Fig. 2b). The mirror mounted in the narrow passage was set at an oblique angle (45 degrees), resulting in a mirrored view of the fish from above (Fig. 2b,c,d). We recorded our videos at 30 fps with a high-resolution digital B/W video camera Kodak Megaplus ES 1.0 (Eastman Kodak Company, Rochester, NY, USA). Each frame contained an image of all fish in the narrow passage from the side and from above. The 3D positional data of individual fish (in mm) were obtained by tracking their snout and the centre of mass (at its greatest height and width) manually on a computer screen during frame-by-frame movie analysis (Fig. 2c). The centre of mass indicated the location of the fish and its direction was given by the direction of the snout tip. The spatial XYZ coordinates of individuals were obtained by combining the measurement of their position in side view (XZ-plane) and in the mirrored view from the top (XY-plane, Fig. 2d). These values we corrected for parallax distortion because of depth of field. The average systematic error that remained was calculated as being max 2% per axis; thus, it is max 3.5% per measurement of the three-dimensional position of an individual. This is well within statistical boundaries. To calibrate the positional data measured in pixels in the video to those in mm in

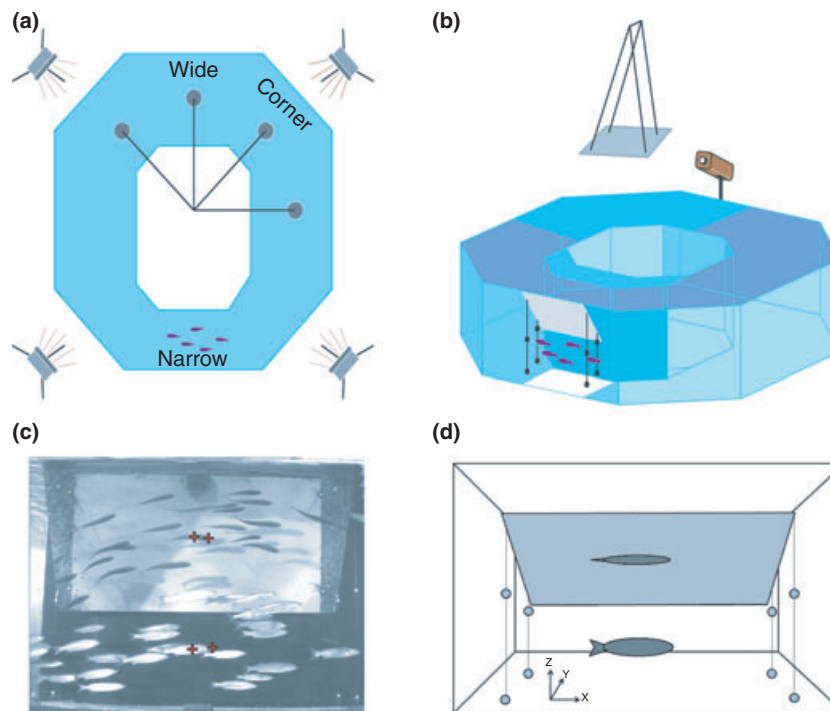


Fig. 2: The tank in reality. (a) Top view, (b) Three-dimensional view. (c) Photograph of a school passing through the narrow passage, (d) Schematic representation of a fish in the narrow passage. (a, b) Front: narrow passage. Back: wide passage. Note that we name the shorter sides, the corners. In (a) Four halogen flood lights are located in each corner. Four dark grey dots connected by lines indicate the four cameras used to film the trajectory of the school. In (b) In the narrow passage, the white hanging rectangle above the fish represents the mirror, the black lines and dots represent the threads with beads (for a photo see Fig. 2c and for an enlarged view see Fig. 2d). Left corner at the back: the corner where the floater was located. Hanging above the floater is the mirror. (c) In the mirror, we see many fish from above. The four crosses indicate the snout and the centre of mass of a single fish and its reflection in the mirror. Note the white beads and their reflection in the mirror. In (d), we see in a schematic view, one fish from its side and its reflection in the mirror from above and the threads with beads.

the real tank, we used the known positions of white beads hanging from thin nylon wires and forming an elongated cube in the narrow passage (Fig. 2c,d).

Large schools did not fit in the narrow passage and, thus, could not be captured in the field of view of the camera as a whole at one moment. Therefore, large schools were sampled in three separate parts, the front, the middle and the hind part. To match these parts of the school and combine them into positional data of all school members at a certain moment without mixing up or ignoring individuals, we traced each individual's displacements in between the three frames in which we captured the front, middle and rear part of the school. We used this method to calculate nearest neighbour (NND) distance and velocity per fish per time step. Velocity was calculated from the positional changes between two subsequent frames.

In the wide passage and in its adjacent corner, we filmed from above and from the side (Fig. 2a). For accurate observation from above, we removed all surface waves by adding a transparent (Perspex) raft

floating on the water. A surface-reflective mirror mounted above the tank made it possible to film from above. We recorded at 30 fps with two high-resolution digital B/W video cameras from above and aside (Kodak Megaplug ES 1.0). The 2D images from the top view were processed to 2D coordinates using image analysis and a point digitizing tool (Didge 2 beta6). Both planar views were calibrated using a standard ruler glued to the tank wall and floor. The average NND from the top view was corrected for school height by multiplying it with the root mean square of normalised height and width. This assumes a uniform distribution of individuals. Therefore, these 3D positions are less precise than those measured with help of the mirror. School shape was calculated by measuring length and width in these recordings.

We collected data on groups comprising 10 till 60 individuals. Each day, the mullets split up in the schools of different sizes. Therefore, we recorded different numbers of schools per school size. We studied 14 groups of 10 individuals, 13 of 20, 33 of 30, 6 of 40, 18 of 50 and 3 of 60 individuals.

The model

Overview and Design of Behavioural Rules

The model consists of artificial fish that move in an octagonal 3D tank identical to the real one (Fig. 2a,b). The movement behaviour of each individual is given in three dimensions (Fig. 3a) and it is based on its social reaction to its neighbours and on its avoidance of collision with the walls of the tank. The social interactions of an individual with others differ according to the position and direction of its neighbours in three overlapping behavioural zones (Fig. 3b). An individual simultaneously moves to others in its cohesion zone, aligns its movement to individuals that are at an intermediate distance from it (in its alignment zone) and separates from others that are close by in its zone of separation. An individual cannot perceive others through walls, and the distance over which it perceives other group members decreases with local density to reflect the fact that individuals are influenced only by those they *can* perceive: when the local density is higher, their perception shrinks to a shorter distance than when it is lower. Note that this adaptable range of perception is supported by empirical evidence for starlings (Ballerini et al. 2008a).

The avoidance of walls is based on two forces that depend on the distance of an individual to the wall. When the individual is still far away from the wall, it will anticipate the wall by aligning its movement to that of the wall (Huth & Wissel 1993), but if it is very close to the wall, it experiences a repulsion from it (Hensor et al. 2005; Doustari & Sannomiya 1995; Hoare et al. 2004; Gautrais et al. 2008). Similarly, the individual avoids collision with the bottom of the tank and the surface.

An individual travels at cruise speed (Videler 1993). It can deviate from this speed by slowing down to avoid bumping into others and by speeding up if it is strongly attracted to others further in front.

The actual behaviour of individuals results from the combination of coordinated movement and wall avoidance. As there is no ethological theory to represent intentions, we calculated the behavioural tendency of an individual as a Newtonian net steering force that consists of the sum of the three ‘social’ steering forces (separation, alignment and cohesion), the two forces to avoid collision with the walls (wall alignment and wall repulsion) plus additional terms for the control of speed.

The model is implemented in C++.

Details of Behavioural Rules

Each individual is characterised by its position, r , its velocity, v , and its orientation in space. Its orientation is indicated through its local coordinate system with its forward direction, e_x , its sideward direction, e_y , and its upward direction, e_z . The individual changes its orientation by rotations around these three principal axes, e_x , e_y and e_z (*roll*, *pitch* and *head*) like in the model by Reynolds (1987) (Fig. 3a).

Its position depends on its former position and its velocity (Eq. 1). Its actual velocity depends on its former velocity, its mass and a net force acting on it which depends on e.g. its social interaction and wall avoidance (Eq. 2). We calculate its position and velocity at the end of each time step Δt by applying Euler integration:

$$r_i(t + \Delta t) = r_i(t) + v_i(t + \Delta t) \cdot \Delta t \tag{1}$$

$$v_i(t + \Delta t) = v_i(t) + \frac{1}{m} \cdot f_{neti} \Delta t \tag{2}$$

Here, r_i is the location of individual i , v_i is its velocity, m its mass and Δt is the update time. At each time step Δt , the position and velocity of all individuals are synchronously updated.

The net force f_{neti} on an individual is updated at each time step Δu . To reflect the reaction time of fish, this time step is longer than that of integration

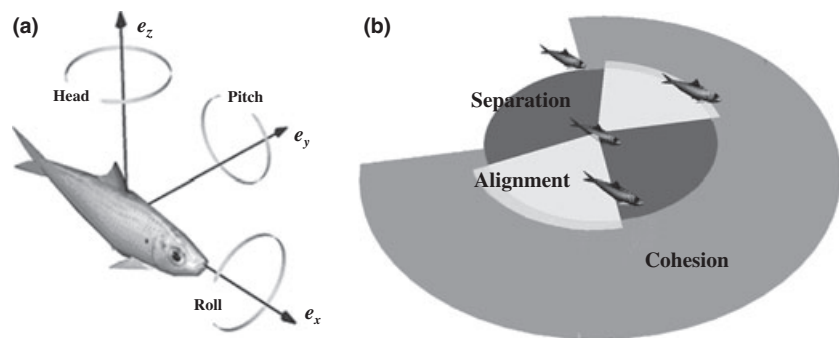


Fig. 3: The local coordinate system (a) and the behavioural zones of the social reactions (b). For explanation, see text.

Δt . It depends on its social interactions, wall avoidance, actual velocity, the stabilisation of its orientation and a random factor (Eq. 3). It is the sum of nine different forces:

$$f_{neti} = f_{si} + f_{ai} + f_{ci} + f_{wai} + f_{wri} + f_{speedi} + f_{pci} + f_{rci} + f_{\zeta i} \quad (3)$$

As will be explained in detail later in the text, f_{si} , f_{ai} and f_{ci} represent the three social forces of, respectively, separation, alignment and cohesion with their interaction partners, f_{wai} and f_{wri} the two forces of reaction to the walls, respectively, of aligning to it and being repulsed by it, f_{speedi} the force that returns individuals to cruise speed, f_{pci} that makes them move horizontally, f_{rci} that keeps them from rolling over their shoulder and $f_{\zeta i}$ a random force. If this force f_{neti} exceeds a magnitude f_{max} it is rescaled to f_{max} , thus limiting the maximum acceleration to 2.5 body lengths per second (for default parameters, see Table 1).

As to the social interaction, the radius of social interaction of each individual is adapted to the density of the surrounding groupmembers. At a very high density, it may even shrink below that of the default range of alignment (and thus shorten the range of alignment too) but it cannot become smaller than the separation range R_{min} . The new perception radius, $R(t+\Delta t)$, is calculated as linear interpolation of the current radius $R(t)$ and a density-dependent term:

$$R'_i = R_{max} - w_n \cdot n(t)$$

$$R_i(t + \Delta t) = \max\{R_{min}, (1 - s) \cdot R(t) + s \cdot R'_i\}; \quad (4)$$

$$s = s_{int} \cdot \Delta t$$

where $n(t)$ is the number of perceived neighbours at time t . The parameter w_n indicates the influence of a single neighbour, and s_{int} controls the smoothness of the radius adaptation.

For two of the social interactions, cohesion and alignment (Fig. 3b), the individual has a blind zone at the back (Couzin et al. 2002). For alignment, it also has a blind angle at the front because alignment is supposed to be mediated by perception through the lateral lines and these are mostly located at the side (Partridge 1981).

To prevent colliding with the n_s , others that are in its separation zone, individual i perceives a steering force f_{si} to move in the opposite direction of the average direction of others inversely weighted by

Table 1: Default parameters.

Parameter	Unit	Symbol	Value(s) explored
Number of individuals	1	N	10-60
Integration time step	S	Δt	0.005
Response latency time step	S	Δu	0.05
Adjustable radius of perception			
Neighbour weight	BL	w_n	1
Interpolations factor	1/s	s_{int}	1
Separation			
Zone radius	BL	R_{min}	1.8
Blind angle back	Degrees	–	0
Weight	BL BM/s ²	w_s	15
Alignment			
Maximum zone radius	BL	–	2 (adaptive)
Frontal blind angle	Degrees	–	45
Blind angle back	Degrees	–	53
Weight	BL BM/s ²	w_a	8
Cohesion			
Maximum zone radius	BL	R_{max}	12 (adaptive)
Blind angle back	Degrees	–	45
Weight	BL BM/s ²	w_c	10
Wall interaction			
Alignment travelling time	S	t_{wa}	3
Alignment weight	BM/s	w_{wa}	2
Repulsion distance	BL	D_{wr}	0.7 [vertical: 2.0]
Repulsion weight	BL BM/s ²	w_{wr}	1 [vertical: 1.5]
Cruise speed	BL/s	v_0	2
Max. speed	BL/s	–	4
Min. speed	BL/s	–	0.5
Relaxation time acceleration	S	τ_a	1/10
Relaxation time deceleration	S	τ_d	1/20
Pitch control	BL ² BM/s ²	w_{pc}	5
Roll control	BL ² BM/s ²	w_{rc}	0.5
Random noise	BL ² BM/s ²	$\ f_{\zeta}\ $	1
Max. force	BL ² BM/s ²	f_{max}	2.5

the quadratic distance at which it perceives the others:

$$d_{si} = -\frac{1}{n_s} \sum_{j=1}^{n_s} \frac{r_{ij}}{\|r_{ij}\|^2}; \quad f_{si} = w_s \cdot \frac{d_{si}}{\|d_{si}\|} \quad (5)$$

where, d_{si} is the preferred direction of separation, and $r_{ij} = (r_j - r_i)$ is the vector pointing towards neighbour j . The influence of a neighbour diminishes quadratically with its distance to the acting agent, as has been used by others (Reynolds 1987; Reuter & Breckling 1994; Kunz & Hemelrijk 2003; Hemelrijk & Kunz 2005).

As regards the n_a neighbours in its alignment zone, individual i perceives a steering force, f_{ai} , to align with their average forward direction:

$$d_{ai} = \frac{1}{n_a} \sum_{j=1}^{n_a} e_{xj} \quad ; \quad f_{ai} = w_a \cdot \frac{d_{ai} - e_{xi}}{\|d_{ai} - e_{xi}\|} \quad (6)$$

d_{ai} is the alignment direction of individual i , and e_{xi} and e_{xj} are the vectors indicating the forward direction of individuals i and j .

Further, individuals are cohering by a steering force f_{ci} to the centre of gravity (i.e. the average x , y , z position) of the group of n_c individuals located in their cohesion area:

$$d_{ci} = \frac{1}{n_c} \sum_{j=1}^{n_c} \frac{r_{ij}}{\|r_{ij}\|} \quad ; \quad f_{ci} = w_c \cdot \frac{d_{ci}}{\|d_{ci}\|} \quad (7)$$

Here, the calculation of the directions of alignment, d_{ai} , and of coherence, d_{ci} , are identical to those of the model by Couzin et al. (2002).

As regards reactions to the wall, at a certain travelling distance from the wall, individuals start to align with it to prevent colliding with it. The travelling distance is computed by dividing the individual’s velocity by its distance to the wall it approaches. If this quotient is smaller than a threshold, the individual will turn to align with the wall. The angle over which the individual turns decreases with its travelling distance from the wall:

$$f_{wai} = \begin{cases} \pm w_{wa} \cdot \frac{v_i}{D_i} \cdot e_{yi} & ; \quad D_i/v_i < t_{wa} \\ 0 & ; \quad \text{else} \end{cases} \quad (8)$$

Here, w_{wa} is the weight of wall alignment, v_i is the speed of individual i , D_i is its distance to the wall in the forward direction, e_{yi} is its sideward direction, t_{wa} is the threshold for starting wall alignment. The sign is chosen in such a way that the individual turns away from the wall it heads towards.

To prevent that fish ignore the wall at their side when they are close to it, we made individuals experience a tendency to move away orthogonally from the wall, by a force f_{wri} . Individuals experience this force when they are closer than a fixed threshold distance from it.

$$f_{wri} = \begin{cases} w_{wr} \cdot N_{\theta} & ; \quad D_{oi} < D_{wr} \\ 0 & ; \quad \text{else} \end{cases} \quad (9)$$

Here, w_{wr} is the weight of repulsion from the wall. N_{θ} is a vector pointing orthogonally from this wall into the water, D_{oi} is the distance of the individual to this wall, and D_{wr} is the threshold distance. We applied the same rule (with different parameter values) to the vertical interaction with the bottom of the tank and with the water surface.

Together, the social tendencies plus the forces to avoid the wall may cause individuals to slow down (e.g. to avoid collisions) or to speed up (e.g. to catch up). However, each individual prefers to swim at cruise speed v_0 and deviations from this are reduced by a compensating force (Helbing & Molnar 1995):

$$f_{speedi} = \frac{1}{\tau} (v_0 - v_i) e_{xi} \quad (10)$$

where the ‘relaxation time’ τ is the characteristic time scale for the return to cruise speed. The value of the parameter τ becomes either $\tau = \tau_a$ or $\tau = \tau_d$ if the individual is currently slower or faster than cruise speed, respectively (see Parametrization, Table 1).

During migration, real fish do not show large pitch angles over longer periods and they virtually never roll. To stabilise the three-dimensional orientation of the individuals, we use a pendulum-like method in which we rotate the individuals back into a horizontal plane by applying the following correcting forces:

$$f_{pci} = -w_{pc}(e_{xi} \cdot z) z; \quad f_{rci} = -w_{rc}(e_{yi} \cdot z) z \quad (11)$$

Here, f_{pci} is the force to control the pitch using a weight of w_{pc} , and f_{rci} is the force to control rolling by a weight w_{rc} , z is the global up-direction. The forward direction is e_x and e_y is the sideward direction.

A random component, $f_{\zeta i}$, is added to the sum of these forces to reflect that decision-making in animals is subject to stochastic effects (such as sensory error and undefined motivational influences).

Parameterization, Initial Conditions and Experiments

While the positions and movements of the individuals are continuously changing in reality, the reactions of individuals to others and to the walls suffer a delay depending on the specific reaction time of the species. To reflect this, we used two time steps: a small time step for the integration of the positions and movements of the individuals Δt , i.e. of 0.005 s, and a longer time step, Δu , i.e. 0.05 s, for updating the net force. This longer update time represents the reaction time of the individuals to others and to the walls or the response latency of shoaling fish to external stimuli (Partridge & Pitcher 1980; Couzin et al. 2002).

Parameters in the model are set to resemble empirical data: The tank is of the same size and shape as the one we used for our experiments with

mulletts (Fig. 2a,b). The unit of length in the model is one body length, BLU, which represents the average body length of mulletts in our empirical study, i.e. 15 cm. In the model, we gave the force for wall alignment and wall repulsion ($w_{wa} = 2$, $w_{wr} = 1$) a smaller weight than the social separation force ($w_s = 15$) because in our empirical study, mulletts came on average closer to walls than to their school members (closest distance to walls was 0.3 BL and to school members was 0.7 BL). To set the free parameters in the model, we chose arbitrarily the largest school size of our empirical data, namely of 60 individuals. When it appeared that the avoidance of the walls slowed down the individuals, we compensated this by omitting the blind angle at the back creating separation all around (similar to Couzin et al. 2002) and we run all simulations without a blind angle of separation. We studied a cruise speed of 2 BL/s because it resembles that of our mulletts of 1.8 BL/s and it is the same as in our former model (to which we compare in the discussion) (Hemelrijk & Hildenbrandt 2008). Because the parameterization of our model is specific to the specific tank and the specific species (mulletts), sensitivity analysis is out of scope of our work. Because we approximately tuned parameters to get behaviour of real fish, there is no danger of overfitting.

At the start of a run, single individuals were located in the centre of the aquarium oriented in similar directions. To eliminate traces of this initial condition, the simulation was run for five circulations before data were collected.

We studied similar school sizes to those in the empirical study, i.e. of 10, 20, 30, 40, 50 and 60 individuals.

Measurements and Statistical Analysis of the Model

To calculate the statistical measures from the 3D positions, we use the same program for the model as for the empirical data.

Because of the shape of the tank, the shape of the school is bent. Therefore, we quantified its shape using a ring-shaped bounding box. Its outer radius (taken from the centre of the tank) included the outermost individual of the school, the innermost ring passed through the innermost individual. At the front and back, the bounding box extended from the place of the frontal and rearward individuals.

The length of the school was calculated as the length of the arc that passed through the corrected geometrical centre of the school. The width of the

school was measured as the radial distance between the inner and outer ring. The elongation of the school is given by the ratio of its length divided by its width (Kunz & Hemelrijk 2003; Hemelrijk & Kunz 2005; Hemelrijk & Hildenbrandt 2008). The 'spinal' centre of mass was measured along the midline of the school.

We calculate the average nearest neighbour distance of the school as the average of the distance of each individual to its closest neighbour. This measure of density we prefer to that of the number of individuals per unit of volume because at the border of the school, the volume cannot be measured with precision because of the difficulty of encompassing it precisely in a three-dimensional hull or envelope. Consequently, when there is relatively more border area (such as is the case for smaller schools), the density will be underestimated (Ballerini et al. 2008b).

We also investigate whether in the interior of the school the nearest neighbour distance increases with group size. Individuals are considered to be located in the interior of the school if they are more or less at all sides surrounded by others. This is indicated by a value ranging between 0 and 0.35 for their 'centrality', C_i i.e. the average direction of all group members relative to the focal individual i (Fig. 4a, Hemelrijk 2000; Hildenbrandt et al. in press). To obtain a sufficiently large sample size, we collected 5 min. of data (consisting of 5×60 frames) per group size. In case of small groups, some frames lacked data.

The local polarisation in the narrow passage is computed as the average deviation of the angle between the heading of the individual and the direction to each of its local neighbours (i.e. those partners that are in its adjustable interaction radius). It is not feasible to calculate the global polarisation of the whole group, because the school is bent continuously.

Data were averaged over 30 circulations. Each circulation a single snapshot was taken when the corrected, weighted centre of mass of the school passed the centre of a wide passage, narrow passage and corner. Per circulation we collected a single data point on wide passage, narrow passage and corner.

We used only non-parametric tests and two-tailed probabilities. When comparing nearest neighbour distance, polarisation, and the quotient of length and width of the school by the Wilcoxon matched-pairs signed-ranks test between model and empirical data, we used modelling data on different group sizes in the same proportion as those of the empirical

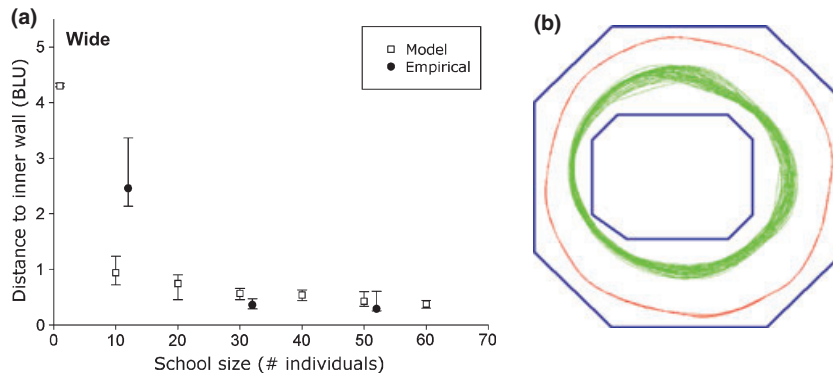


Fig. 4: Group size and distance of fish to the inner wall. (a) Average distance to the inner wall of the three mullets closest to it for different group sizes (median and interquartile) in the wide passage. Closed circle: empirical data, Open square: model data at slow cruise speed. A similar pattern is observed in the narrow passage and in the corner, but quantitative empirical data of this are lacking for the narrow passage. Note that the complete width of the passage is reflected, i.e. 5.5 BLU or 83 cm. Thus, the solitary fish (shown in the model data) swim along the outer wall. (b) The model of individuals in a tank: Trajectories of a solitary fish (outercircles, in red) and a school of 60 fish (innercircles, in green). For explanation, see text.

study. For this, we drew data from specific group sizes in our model randomly.

Results

Validation of the Model

The trajectory of a school both in the model and in the empirical data depend on school size. In real fish and in the model, larger schools (of 20 and more individuals) were closer to the inner wall than the outer wall (Fig. 4a). In the model, this is clearest when comparing the trajectory between a single individual and a school of individuals (Fig. 4b).

We obtained schools with similar NND, speed and polarisation as those of the empirical data in the narrow passage (Wilcoxon matched-pairs signed-ranks test between model and empirical data, $N = 6$, $NND\ T = -8.5$ NS, speed $T = +11$ NS, polarisation, $T = -3$ NS, respectively).

School shape both in our model with tank and in our empirical data appeared to be oblong always (i.e. the ratio of length to width is larger than 1, see Figs 5 and 6).

The similarity between model and empirical data is a good starting point for studying the hypotheses regarding school shape.

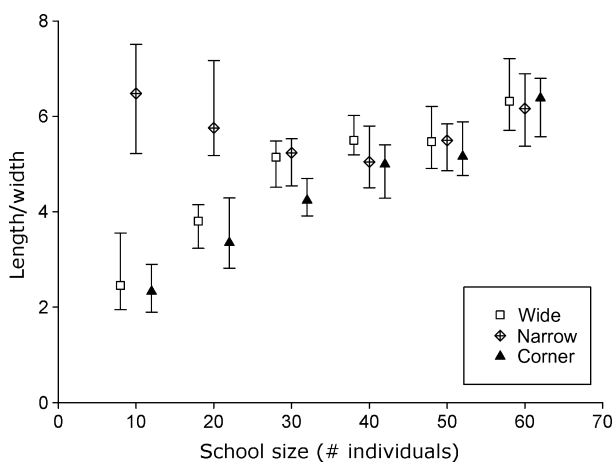


Fig. 5: Ratio of length to width (median and interquartile) vs. school size in model with schools in a tank in wide passage, narrow passage and when moving through the corner. Open squares: wide passage, open diamonds: narrow passage, closed triangles: corner.

Analysis of Effects of Group Size, Speed and Spatial Confinement

The Model with Tank

In our new model with tank, we confirm the two predicted patterns produced by our earlier model (Hemelrijk & Hildenbrandt 2008): (1) larger schools are denser (Fig. 7, Table 2) and (2) they are more oblong (Fig. 5, Table 2), except for individuals in the narrow passage (Fig. 5, Table 2a).

In our theory of the causation of group shape, we explain a decrease in the NND in larger schools as a consequence of the higher attraction among the larger number of individuals. Consequently, we expect that the NND decreases also in the interior of the school. Therefore, we also studied the NND in the interior of the school and how it is affected by group size. The NND in the interior of the school appears indeed to decrease with school size significantly (Fig. 7b, $N = 1463$, $\text{Tau} = -0.39$, $p < 0.0001$).

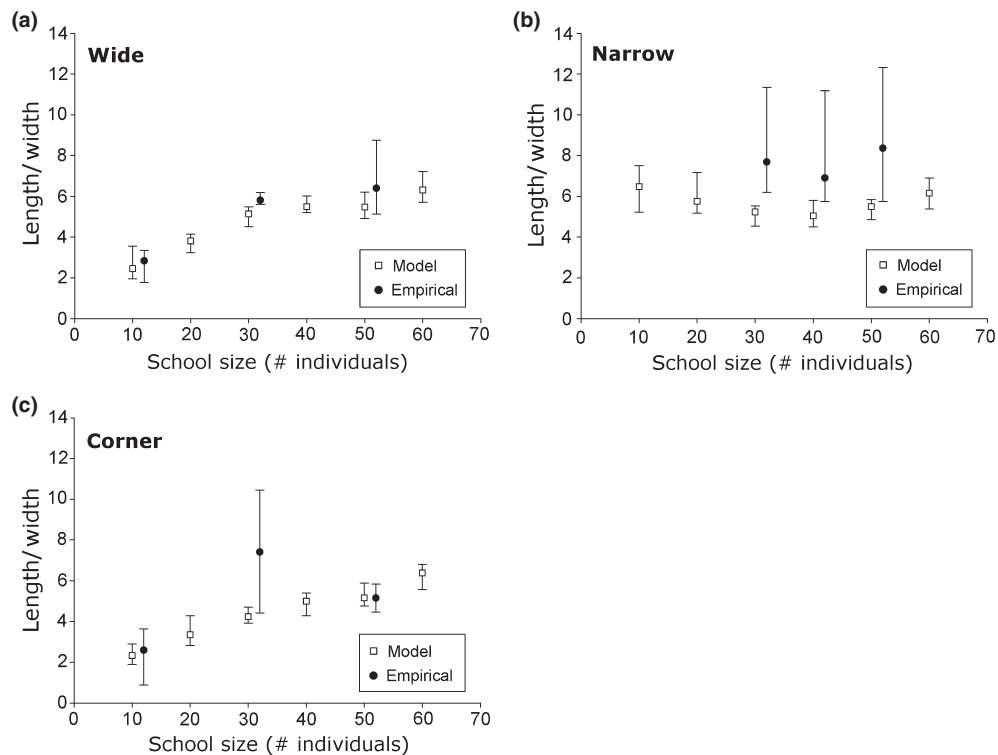


Fig. 6: Ratio of length to width of the school (median and interquartile) vs. school size for model and empirical data (a) in the wide passage, (b) in the narrow passage, and (c) when moving through the corner.

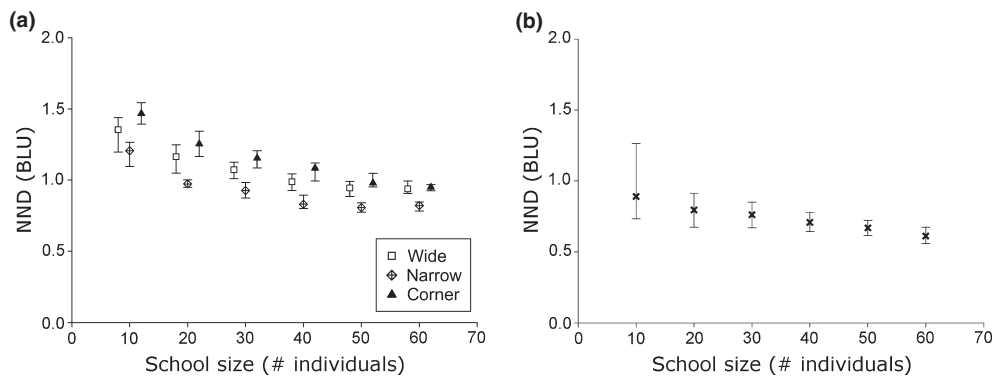


Fig. 7: Average nearest neighbour distance in the school (median and interquartile) vs. school size for model of schools in tank (a) in the whole school in wide passage, narrow passage, and when moving through the corner (b) in the interior of the school during the complete circulation without distinguishing between the different passages.

As regards the effects of wall avoidance, in our model, the nearest neighbour distance (NND) is reduced in schools in the narrow passage compared to that in the wide one (Wilcoxon matched-pairs signed-ranks test, $N = 6$ medians, average NND in wide passage vs narrow, $T = 0$, $p < 0.05$, Fig. 7a), but the shape is similar in both passages (Wilcoxon matched-pairs signed-ranks test, $N = 6$ medians,

length/width in wide passage vs narrow, $T = 7$, NS, Fig. 5).

Empirical Data

In the empirical data, the first two patterns are also confirmed (Fig. 1b): Larger schools are denser in all passages (Fig. 8, Table 2) and they are more oblong

Table 2: Kendall Tau correlations with group size in the three passages of the average nearest neighbour distance and the school shape (length/width). (a) in model with tank and (b) in empirical data

Corr with group size	Tau		
(a) Model	Wide (N = 180)	Narrow (N = 180)	Corner (N = 180)
Average NND	-0.634**	-0.469**	-0.737**
Length/Width	0.595**	0.089 NS	0.678**
(b) Empirical data	Wide (N = 21)	Narrow (N = 44)	Corner (N = 24)
Average NND	-0.373*	-0.627**	-0.516**
Length/Width	0.534**	0.018 NS	0.418**

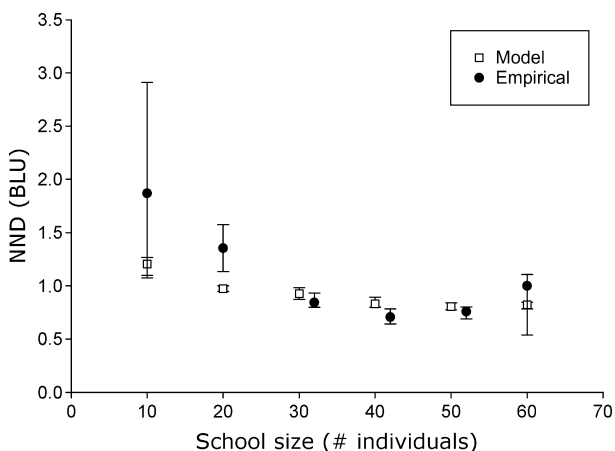
Wide, narrow and corner refer to the passages in the octagonal tank. Two-tailed p values, * = $p < 0.05$, ** = $p < 0.01$. NND, Nearest Neighbour Distance.

except for schools in the narrow passage (Fig. 6, Table 2). We have insufficient data to investigate the internal density, however.

Because of the different precision of measurement of NND in the wide and narrow passages, we cannot compare NND between passages, but the degree to which schools are oblong is similar in the narrow passage and in the wide passage (Mann–Whitney *U*-test for group size of 30 individuals, $N_{\text{wide, narrow}} = 9, 12$, Ranksum = 73, 158, $Z = -1.85$, p (two-tailed) = 0.07 and for group size of 50 individuals $N_{\text{wide, narrow}} = 9, 6$, Ranksum 64, 56, p (two-tailed) = 0.38, Fisher combination test, NS). This resembles the model for different passages in the tank.

Discussion

Our model and empirical data are sufficiently similar to study causation of the oblong shape. For instance,

**Fig. 8:** Average nearest neighbour distance (NND) (median and interquartile) against school size for model and empirical data of schools in the narrow passage of the tank. Open squares: model, closed circle: mullets.

both in our model and in our empirical data, the path length of the school per circulation is shorter for larger schools (Fig. 4a,b). In the model, this arises by self-organisation, because by following the direction adjustment of the preceding individuals, followers in a school will start turning sooner when approaching the corner than individuals at the front of a school. Consequently, a solitary individual turns later than the average individual in a group. Thus, the angle taken through the corner is sharper in a group than for a solitary individual, and the radius of the circulation is shorter. This can be seen as an example of transfer of adaptive information similar to a 'Trafalgar effect' as has been observed in the context of predation (Treherne & Foster 1981).

Our results support the theory that in a tank, both in a model and in reality, the oblong shape of a school of fish may indeed develop from collision avoidance among group members while travelling in a coordinated school. We have shown two things. First, we have demonstrated the development of an oblong school shape in both, the new model in which schools are confined to a tank and in the empirical data of schools of mullets. Second, as regards the causation of an oblong shape (Kunz & Hemelrijk 2003; Hemelrijk & Kunz 2005; Hemelrijk & Hildenbrandt 2008), the supposed interrelationships between group size and group shape as well as group size and nearest neighbour distance are confirmed in both, models and empirical data (hypotheses 1 and 2, Fig. 1b).

Note that in larger schools in our model, the average nearest neighbour distance is smaller, not only on average in the complete school, but also in its interior. This confirms our explanation that the increase in density with school size may be because of the greater attraction among the higher number of individuals of a larger school. Thus, the increase in density with school size in our model is not merely because of the statistical border effect (Stoyan & Stoyan 1994). This confirms the results of our model of free-swimming fish (Hemelrijk & Hildenbrandt 2008) in which we also reported that density in the interior of the school increased with the number of school members.

Further, as to the absence of the effects of confinement in space on school shape, a greater difference in spatial constraint may be needed. Indeed, if we compare density and shape in our model of schools in a tank to our former model with schools swimming freely (Hemelrijk & Hildenbrandt 2008), nearest neighbour distance appears smaller in the tank (Wilcoxon matched-pairs signed-ranks test, $N = 6$

medians, free vs wide $T = 0$, $p < 0.05$, free vs narrow same result) and school shape is more oblong (Wilcoxon matched-pairs signed-ranks test, $N = 6$ medians, wide vs free $T = 0$, $p < 0.05$, narrow vs free same result). For a comparison with schools in open water, however, empirical data are needed still.

In future, we intend to find out more about the question how school shape is affected by spatial confinement, school size and also speed. As regards spatial confinement, we plan to compare schools in our tank with those in nature and with those in the other tanks of different sizes and shapes. Regarding school size, we will study additional school sizes of 20, 40 and 60 mullets to clarify why in the narrow passage in slow schools there is no correlation between group size and the degree of elongation. Regarding speed, we will analyse the shape of schools of slowly swimming mullets vs. a similar species with a greater cruise speed.

Note that we combine a theoretical and an empirical study of the three-dimensional positions of individuals for schools of fish that are relatively large. The two former studies of three-dimensional position that combined theory and empiry were confined to five bitterlings only, which were studied regarding the trajectory of the school and the correlation in speed among the individuals (Doustari & Sannomiya 1995) and schools of eight Danios, which were studied regarding the interconnection between density and speed (Viscido et al. 2004). Purely empirical studies of the 3D position of individuals concerned somewhat larger schools, but these were still relatively small, for instance consisting of up to 30 individuals (Partridge & Pitcher 1980).

As to the adaptive benefits of the oblong shape of fish schools, our study is not informative. It shows, however, that there is no need of a functional explanation of the oblong shape. It develops merely as a side effect of slowing down to avoid collisions. It is possible that the oblong shape is adaptive, e.g. when predators attack at the front (Bumann et al. 1997), but it can also be maladaptive when predators attack from the side, because the side is clearly visible. Fish schools may meet with several predators that attack at different locations possibly in different periods (seasons, years) or even in the same period of the year. This could result in a diffusive or neutral selection pressure on the shape of a school. This argument resembles that of Jovani & Grimm (2010) in a modelling study of the synchronisation of breeding in colonies of birds. The authors showed that this synchronisation may result from a local mechanism, namely because

individuals avoid to lay eggs close to females that are agitated. They argued that synchronisation may be effective against a satiable territorial predator, but that it is disastrous against grouping predators that are attracted by the bursts of high numbers of chickens produced in such colonies.

It should be noted that our explanation of the causation of the shape of a moving group may not apply to very large groups nor to other kinds of locomotion (e.g. flying of starlings) because in these cases, the shape is not oblong. The shape of schools with more than 2000 individuals becomes difficult to classify because of their irregular border, both in our former model (Hemelrijk & Hildenbrandt 2008) and in real schools of fish (Gerlotto & Paramo 2003; Gerlotto et al. 2004). The regulation of the shape of these very large schools asks for a separate investigation combining an empirical and a modelling study. Further, it appears that in case of another kind of locomotion, such as flying, the spatial confinement to circling above a sleeping site (during aerial displays of starlings) may outweigh the process leading to an oblong shape and may result in shapes that are highly variable over time and between flocks (Hildenbrandt et al. in press).

Of course, the individuals in our model by no means represent the complexity of that of real fish as this is not the aim of our study. The complexity of our model has been tailored to the questions we pose. In studies of schooling fish by others, both have been used: models of schooling that are more complex (Barbaro et al. 2009) and that are simpler than our model presented here (Vicsek et al. 1995).

In sum, we show that the models of self-organised schooling are useful to increase our understanding of the shape of schools of real fish. Both our theoretical and our empirical study support the hypothesis that the oblong shape of moving groups of fish is a consequence of the avoidance of collision with group members during coordinated movement.

Acknowledgements

We thank the students that worked on earlier setups of the experiments with mullets (Vincent Boer, Arend van Dijk, Marielle de Groot and Maartje Giesbers) and earlier versions of the model (Thijs Janzen). We thank Jos de Wiljes for taking care of the animals. Our work was partly financed by a grant from the STREP-project 'StarFlag' in the NEST-programme of 'Tackling complexity in science' of 6th European framework awarded to Hemelrijk and by financial support by NWO programme Cogni-

tion to Charlotte Hemelrijk in the form of a grant for a pilot project, number 051.07.006. We thank Irene Giardina and Volker Grimm for their valuable comments on an earlier version.

Literature Cited

- Axelsen, B. E., Anker-Nilssen, T., Fossum, P., Kvamme, C. & Nottestad, L. 2001: Pretty patterns but a simple strategy: predator-prey interactions between juvenile herring and Atlantic puffins observed with multibeam sonar. *Can. J. Zool.* **79**, 1586—1596.
- Ballerini, M., Cabibbo, N., Candelier, R., Cavagna, A., Cisbani, E., Giardina, I., Lecomte, V., Orlandi, A., Parisi, G., Procaccini, A., Viale, M. & Zdravkovic, V. 2008a: Interaction ruling animal collective behaviour depends on topological rather than metric distance: evidence from a field study. *Proc. Natl. Acad. Sci. USA* **105**, 1232—1237.
- Ballerini, M., Cabibbo, N., Candelier, R., Cavagna, A., Cisbani, E., Giardina, I., Orlandi, A., Parisi, G., Procaccini, A., Viale, M. & Zdravkovic, V. 2008b: Empirical investigation of starling flocks: a benchmark study in collective animal behaviour. *Anim. Behav.* **76**, 201—215.
- Barbaro, A., Einarsson, B., Birnir, B., Sigurðsson, S., Valdimarsson, H., Pálsson, Ó. K., Sveinbjörnsson, S. & Sigurðsson, P. 2009: Modeling and Simulations of the Migration of Pelagic Fish. *ICES J. Mar. Sci.* **66**, 826—838.
- Bazazi, S., Buhl, J., Hale, J. J., Anstey, M. L., Sword, G. A., Simpson, S. J. & Couzin, I. D. 2008: Collective Motion and Cannibalism in Locust Migratory Bands. *Curr. Biol.* **18**, 735—739.
- Becco, C., Vandewalle, N., Delcourt, J. & Poncin, P. 2006: Experimental evidences of a structural and dynamical transition in fish school. *Physica A* **367**, 487—493.
- Biro, D., Sumpter, D. J. T., Meade, J. & Guilford, T. 2006: From compromise to leadership in pigeon homing. *Curr. Biol.* **16**, 2123—2128.
- Breder, C. M. 1954: Equations Descriptive of Fish Schools and Other Animal Aggregations. *Ecology* **35**, 361—370.
- Breder, C. M. 1959: Studies on social groupings in fish. *Bull. Am. Mus. Nat. Hist.* **117**, 397—481.
- Breder, C. M. 1976: Fish Schools as Operational Structures. *Fish. Bull.* **74**, 471—502.
- Buhl, J., Sumpter, D. J. T., Couzin, I. D., Hale, J. J., Despland, E., Miller, E. R. & Simpson, S. J. 2006: From disorder to order in marching locusts. *Science* **312**, 1402—1406.
- Bumann, D., Krause, J. & Rubenstein, D. 1997: Mortality risk of spatial positions in animal groups: the danger of being in the front. *Behaviour* **134**, 1063—1076.
- Couzin, I. D. & Krause, J. 2003: Self-organization and collective behavior in vertebrates. In: *Advances in the Study of Behavior*, Vol. **32** (Slater, P., Rosenblatt, J., Snowdon, C., Roper, T., eds). Elsevier, San Diego, pp. 1—75.
- Couzin, I. D., Krause, J., James, R., Ruxton, G. D. & Franks, N. R. 2002: Collective memory and spatial sorting in animal groups. *J. Theor. Biol.* **218**, 1—11.
- Couzin, I. D., Krause, J., Franks, N. R. & Levin, S. A. 2005: Effective leadership and decision-making in animal groups on the move. *Nature* **433**, 513—516.
- Cushing, D. H. & Harden-Jones, F. R. 1968: Why do fish school? *Nature* **218**, 918—920.
- Doustari, M. A. & Sannomiya, N. 1995: A simulation study on schooling behaviour of fish in a water tank. *Int. J. Systems Sci.* **26**, 2295—2308.
- Faria, J. J., Codling, E. A., Dyer, J. R. G., Trillmich, F. & Krause, J. 2009: Navigation in human crowds; testing the many-wrongs principle. *Anim. Behav.* **78**, 587—591.
- Gautrais, J., Jost, C., Soria, M., Campo, A., Motsch, S., Fournier, R., Blanco, S. & Theraulaz, G. 2008: Analyzing fish movement as a persistent turning walker. *J. Math. Biol.* **58**, 429—445.
- Gerlotto, F. & Paramo, J. 2003: The three-dimensional morphology and internal structure of clupeid schools as observed using vertical scanning multibeam sonar. *Aquat. Living Resour.* **16**, 113—122.
- Gerlotto, F., Castillo, J., Saavedra, A., Barbieri, M. A., Espejo, M. & Cotel, P. 2004: Three-dimensional structure and avoidance behaviour of anchovy and common sardine schools in central southern Chile. *ICES J. Mar. Sci.* **61**, 1120—1126.
- Grünbaum, D. 1998: Schooling as a strategy for taxis in a noisy environment. *Evol. Ecol.* **12**, 503—522.
- Gueron, S. & Levin, S. A. 1993: Self-organisation of front patterns in large Wildebeest herds. *J. Theor. Biol.* **165**, 541—552.
- Hamilton, W. D. 1971: Geometry for the selfish herd. *J. Theor. Biol.* **31**, 295—311.
- Helbing, D. & Molnar, P. 1995: Social force model for pedestrian dynamics. *Phys. Rev. E Stat. Phys. Plasmas Fluids Relat. Interdiscip. Topics* **51**, 4282—4286.
- Hemelrijk, C. K. 2000: Towards the integration of social dominance and spatial structure. *Anim. Behav.* **59**, 1035—1048.
- Hemelrijk, C. K. & Hildenbrandt, H. 2008: Self-organized shape and frontal density of fish schools. *Ethology* **114**, 245—254.
- Hemelrijk, C. K. & Kunz, H. 2005: Density distribution and size sorting in fish schools: an individual-based model. *Behav. Ecol.* **16**, 178—187.
- Hensor, E., Couzin, I. D., James, R. & Krause, J. 2005: Modelling density dependent fish shoal

- distributions in the laboratory and the field. *Oikos* **110**, 344–352.
- Hildenbrandt, H., Carere, C. C. & Hemelrijk, C. K. (in press): Self-organised complex aerial displays of thousands of starlings: a model. *Behav. Ecol.*, in press.
- Hoare, D. J., Couzin, I. D., Godin, J. G. J. & Krause, J. 2004: Context-dependent group size choice in fish. *Anim. Behav.* **67**, 155–164.
- Huse, G., Railsback, S. & Ferno, A. 2002: Modelling changes in migration pattern in herring: collective behaviour and numerical domination. *J. Fish Biol.* **60**, 571–582.
- Huth, A. & Wissel, C. 1992: The Simulation of the Movement of Fish Schools. *J. Theor. Biol.* **156**, 365–385.
- Huth, A. & Wissel, C. 1993: The analysis of behaviour and the structure of fish schools by means of computer simulations. *Comm. Theor. Biol.* **3**, 169–201.
- Huth, A. & Wissel, C. 1994: The simulation of fish schools in comparison with experimental data. *Ecol. Modell.* **75/76**, 135–145.
- Jovani, R. & Grimm, V. 2010: Breeding synchrony in colonial birds: from local stress to global harmony. *Proc. R. Soc. Lond., B, Biol. Sci.* **275**, 1557–1564. doi: 1510.1098/rspb.2008.0125.
- Keenleyside, M. H. A. 1955: Some aspects of schooling behaviour in fish. *behaviour* **8**, 183–248.
- Krause, J. & Ruxton, G. D. 2002: *Living in groups*. Oxford Univ. Press, Oxford.
- Kunz, H. & Hemelrijk, C. K. 2003: Artificial fish schools: collective effects of school size, body size, and body form. *Artificial Life* **9**, 237–253.
- Nursall, J. R. 1973: Some Behavioral Interactions of Spottail Shiners (*Notropis hudsonius*), Yellow Perch (*Perca flavescens*), and Northern Pike (*Esox-Lucius*). *J. Fish. Res. Board Can.* **30**, 1161–1178.
- Parrish, J. K. & Viscido, S. V. 2005: Traffic rules of fish schools: A review of agent-based approaches. In: *Self-organisation and the evolution of social behaviour* (Hemelrijk, C. K., ed). Cambridge Univ. Press, Cambridge, UK, pp. 50–80.
- Partridge, B. L. 1980: Effect of School Size on the Structure and Dynamics of Minnow Schools. *Anim. Behav.* **28**, 68–77.
- Partridge, B. L. 1981: Lateral line function and the internal dynamics of fishschools. In: *Hearing and sound communication in fishes* (Tavolga, W. N., Fay, R. R. & Popper, A. N., eds). Springer, Berlin, pp. 515–521.
- Partridge, B. L. & Pitcher, T. J. 1980: The Sensory Basis of Fish Schools - Relative Roles of Lateral Line and Vision. *J. Comp. Physiol.* **135**, 315–325.
- Partridge, B. L., Pitcher, T., Cullen, J. M. & Wilson, J. 1980: The 3-Dimensional Structure of Fish Schools. *Behav. Ecol. Sociobiol.* **6**, 277–288.
- Pitcher, T. J. 1986: Functions of shoaling behaviour in teleosts. In: *The behaviour of Teleost fishes* (Pitcher, T. J., ed). Croom Helm, London, pp. 294–337.
- Radakov, D. V. 1973: *Schooling in the ecology of fish*. John Wiley and Sons, New York.
- Reuter, H. & Breckling, B. 1994: Selforganization of Fish Schools - an Object-Oriented Model. *Ecological Modelling* **75**, 147–159.
- Reynolds, C. W. 1987: Flocks, herds and schools: a distributed behavioral model. *Computer Graphics* **21**, 25–36.
- Romanczuk, P., Couzin, I. D. & Schimansky-Geier, L. 2009: Collective Motion due to Individual Escape and Pursuit Response. *Phys. Rev. Lett.* **102**, 2–4.
- Simpson, S. J., Sword, G. A., Lorch, P. D. & Couzin, I. D. 2006: Cannibal crickets on a forced March for protein and salt. *PNAS* **103**, 4152–4156.
- Stoyan, D. & Stoyan, H. 1994: *Fractals, Random Shapes and Point Fields: Methods Of Geometrical Statistics*. John Wiley & Sons, Chichester.
- Treherne, J. E. & Foster, W. A. 1981: Group transmission of predator avoidance behaviour in a marine insect: the Trafalgar effect. *Anim. Behav.* **29**, 911–917.
- Vicsek, T., Czirók, A., Ben-Jacob, E., Cohen, I. & Shochet, O. 1995: Novel Type of Phase Transition in a System of Self-Driven Particles. *Phys. Rev. Letters* **75**, 1226–1229.
- Videler, J. J. 1993: *Fish swimming*. Chapman & Hall, London.
- Viscido, S. V., Parrish, J. K. & Grunbaum, D. 2004: Individual behavior and emergent properties of fish schools: a comparison of observation and theory. *Marine Ecology-Progress Series* **273**, 239–249.
- Ward, A. J. W., Sumpter, D. J. T., Couzin, I. D., Hart, P. J. B. & Krause, J. 2008: Quorum decision-making facilitates information transfer in fish schools. *Proceedings of National Academy of Sciences* **105**, 6948–6953.
- Yates, C. A., Erban, R., Escudero, C., Couzin, I. D., Buhl, J., Kevrekidis, I. G., Maini, P. K. & Sumpter, D. J. T. 2009: Inherent noise can facilitate coherence in collective swarm motion. *PNAS* **106**, 5464–5469.

Supporting Information

Additional Supporting Information may be found in the online version of this article:

Video S1. This movie shows that fish in a school travel closer to the inner than the outer wall, whereas single fish do the reverse; Single fish travel closer to the outer wall.

Please note: Wiley-Blackwell are not responsible for the content or functionality of any supporting materials supplied by the authors. Any queries (other than missing material) should be directed to the corresponding author for the article.